Ultrasonics Sonochemistry 72 (2021) 105416

Contents lists available at ScienceDirect

Ultrasonics Sonochemistry

journal homepage: www.elsevier.com/locate/ultson

Ultrasound-assisted rapid hydrothermal design of efficient nanostructured MFI-Type aluminosilicate catalyst for methanol to propylene reaction

Parisa Sadeghpour [a,b], Mohammad Haghighi [a,b,*], Alireza Ebrahimi [a,b]

[a] Chemical Engineering Faculty, Sahand University of Technology, P.O.Box 51335-1996, Sahand New Town, Tabriz, Iran
[b] Reactor and Catalysis Research Center (RCRC), Sahand University of Technology, P.O.Box 51335-1996, Sahand New Town, Tabriz, Iran

ARTICLE INFO

Keywords:
MFI-Type Aluminosilicate
Ultrasound
Rapid Design
Methanol
Propylene

ABSTRACT

The influence of ultrasound-assisted rapid hydrothermal synthesis of aluminosilicate ZSM-5 catalysts was examined in this work. A series of MFI-type nanostructured materials with sonochemical approach and conventional heating were synthesized and evaluated for conversion of methanol to propylene reaction. The prepared samples were tested by characterization analyses such as XRD, FESEM, BET-BJH, FTIR, TPD-NH_3 and TG/DTG. The obtained results confirmed that ultrasound treatment enhanced the nucleation process and crystal growth for ZSM-5 sample synthesized at moderate temperature of 250 °C. Therefore, it was found the formation of pure MFI zeolite with high crystallinity and improved textural, structural and acidic properties for ZSM-5(UH-250) sample compared with the other zeolites. This observation was attributed to the relationship between the perfect crystallization mechanism and catalytic properties, which led to producing an efficient MFI zeolite toward the optimal catalytic performance. In this manner, the methanol conversion and products selectivity of prepared materials were carried out in MTP reaction at 460 °C and atmospheric pressure. The ZSM-5(UH-250) zeolite with slower deactivation regime exhibited the constant level of methanol conversion (84%) and high propylene selectivity (78%) after 2100 min time on stream. Moreover, the synthesis pathway for MFI zeolite at moderate temperature and also deactivation mechanism of improved sample were proposed.

1. Introduction

Today, the most common route to light olefins production is through methanol to olefins reaction (MTO) [1–3]. Light olefins especially consist of ethylene (C_2H_6) and propylene (C_3H_8) [4]. The C_2H_6/C_3H_8 ratio of MTO products can vary considerably depending on the catalyst framework type and as well as reaction conditions [5–7]. In this case, methanol to propylene reaction (MTP) with high amount of propylene production seems to be a suitable strategy by increasing world demand for petrochemical plants [8–10]. MFI-like materials such as aluminosilicate (ZSM-5) are reported to offer certain advantages to obtain the maximum yield of propylene during the MTP process [11–13]. The ZSM-5 framework possesses an anisotropic structure with five-rings which includes cavities and channels by a straight and also a zigzag ten-ring [14–16]. During the MTP reaction, it is suggested that the methanol molecules diffuse in the restricted zigzag channels of the zeolite; react at the cavities on the acid sites, and the products diffuse out through the straight channels [17,18]. The proper pore structure, together with the active acid sites can make aluminosilicate framework an active and shape-selective molecular sieve, particularly for propylene production [19–22]. Due to the relationship between the method of producing aluminosilicate framework and its proportion properties, the recent investigations should be studied the effect of new synthesis strategies on the physico-chemical properties and also catalytic performance of ZSM-5 structure [20,23,24]. The conventional hydrothermal technique has been popularly used for the synthesis of MFI-framework for the past several decades [25]. On the other hand, the novel preparation routes can lead to the specific characteristics that make them effective methods for developing ZSM-5 material [26–28]. According to our pervious study, we prepared nanostructured ZSM-5 catalyst via an effective high temperature hydrothermal synthetic method for the first time [13,29]. It was found that high temperature hydrothermal approach generated MFI molecular sieve in a short crystallization time with such as particular properties, significant cost benefit and high specific activity. Interestingly, it was revealed that the phase purity and crystalline structure of the aluminosilicate final product and also its catalytic performance were strongly dependent on the nucleation and crystal growth [29]. Therefore, it is important to promote a facile route to enhance the

* Corresponding author at: Reactor and Catalysis Research Center, Sahand University of Technology, P.O. Box 51335-1996, Sahand New Town, Tabriz, Iran.
E-mail address: haghighi@sut.ac.ir (M. Haghighi).

https://doi.org/10.1016/j.ultsonch.2020.105416
Received 5 October 2020; Received in revised form 11 November 2020; Accepted 25 November 2020
Available online 7 December 2020

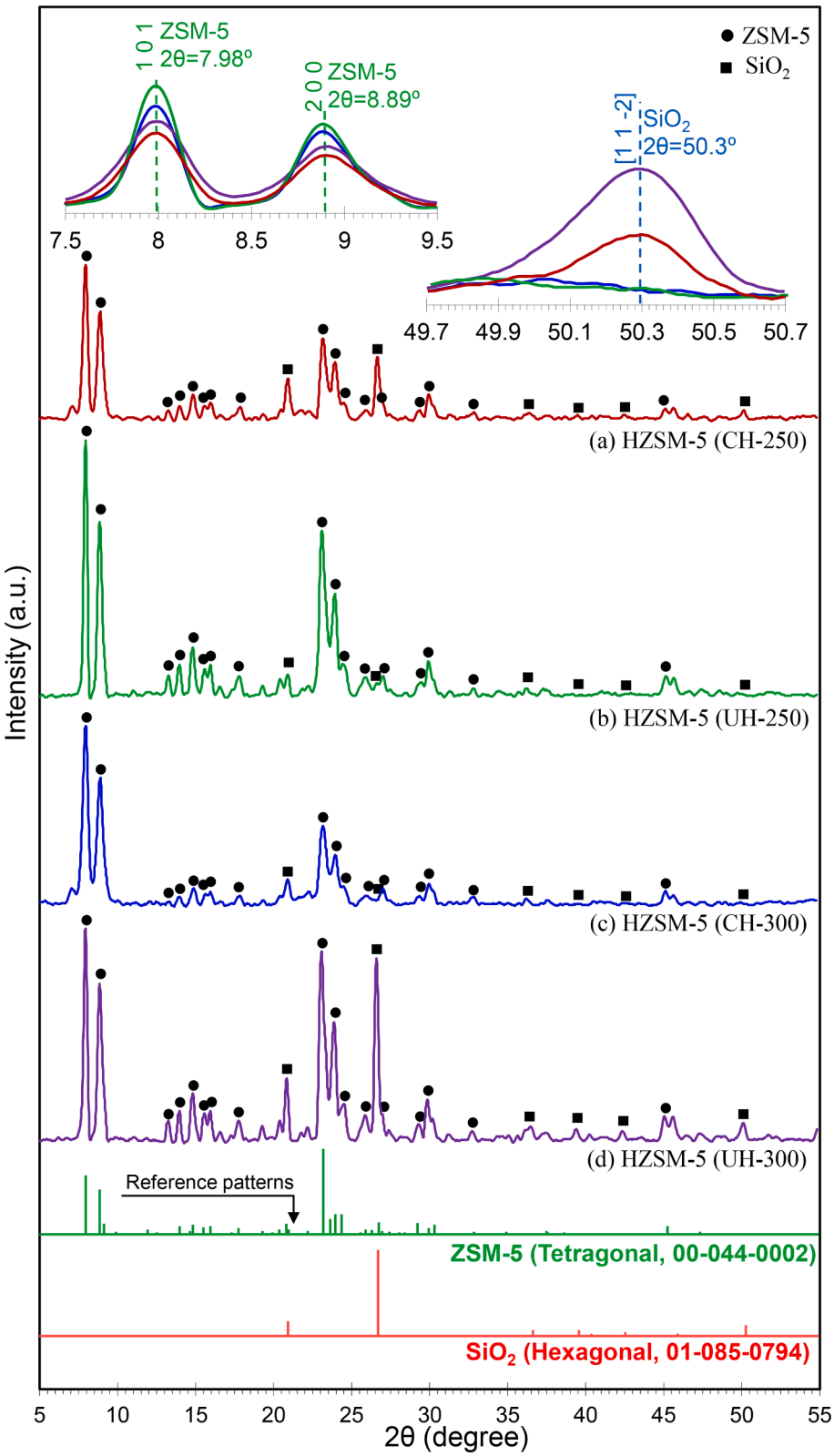

Fig. 1. XRD patterns of efficient nanostructured MFI-type aluminosilicate catalysts: (a) HZSM-5 (CH-250), (b) HZSM-5 (UH-250), (c) HZSM-5 (CH-300) and (d) HZSM-5 (UH-300).

crystallization kinetic. According to the literature, it is found that the application of ultrasound leads to improving influences on induction period, nucleation process, crystal growth rate, crystallite size, morphology, and particle size distribution [27,30,31]. Zhuang et al. [32] synthesized well-ordered ZSM-5 crystals with tunable mesoporosity and high catalytic stability for propylene production from methanol by using a facile ultrasound-assisted approach. Moradiyan et al. [33] reported that utilizing of ultrasound-assisted conventional hydrothermal method for preparation of SAPO-34/ZSM-5 nano composite resulted in a rapid synthesis and formation of dominant mesopore

Table 1
Structural parameters of efficient nanostructured MFI-type aluminosilicate catalyst.

Catalyst	T(°C)	t(h)	UltrasoundIrradiation	S_{BET}[a](m^2/g)	V_{Total}[b](cm^3/g)	Relative Crystallinity[c](%)	
						HZSM-5	SiO_2
HZSM-5 (CH-250)	250	3	No	384	0.2024	52.3	57.1
HZSM-5 (UH-250)	250	3	Yes	397	0.2126	97.2	0.0
HZSM-5 (CH-300)	300	1.5	No	311	0.1639	57.6	7.1
HZSM-5 (UH-300)	300	1.5	Yes	322	0.1804	100	100

[a] Total surface areas were obtained by the BET method.
[b] Total pore volumes were estimated from the adsorbed amount at $P/P_0 = 0.99$.
[c] Relative crystallinity: XRD relative peak intensity for HZSM-5 at $2\theta = 23.2°$ and SiO_2 at $2\theta = 26.7°$.

structure with unique properties. Hence, the use of ultrasound along with high temperature hydrothermal synthesis as alternative routes is proposed for preparation of MFI aluminosilicate framework. Sonochemistry involves high energies and pressure on a short time scale [34]. This can be due to acoustic cavitation which created small bubbles by ultrasonic waves and collapse of micro-bubbles that produced tremendous heat and pressure [27,31,35]. This phenomenon leads to maximum mass transfer in synthesis gel by improving the strength of agitation that has a crucial role for the homogenous dispersion of the components in the gel and as well as nucleation of zeolite and crystal growth [16,36]. As a conclusion, the accelerating influences of both high temperature hydrothermal synthesis and sonochemical methods can cause the formation of efficient and selective ZSM-5 molecular sieve in methanol to propylene reaction.

On the other hand, it is important to find a balance between performance and energy consumption to produce not only energy efficient material but also the reliable product. It seems that the unique combination of new technologies can provide an opportunity to balance the energy consumption, production cost and as well as performance [37,38]}. By using ultrasound-assisted hydrothermal synthesis, the pure and efficient MFI-type aluminosilicate framework can be synthesized at moderate temperature and short time associated with the energetic and economic benefits and also enhanced catalytic performance. Keep those mentioned above in mind, alternative routes of high temperature short time hydrothermal method and ultrasound approach were investigated for ZSM-5 synthesis with MFI crystalline structure. However, several research groups have used ultrasound assisted conventional hydrothermal approach to prepare different zeolites, but there is no open literature on the study of ultrasound assisted high temperature synthesis for MFI zeolite preparation. The synthesized novel catalysts were characterized by several characterization techniques. Moreover, the catalytic behaviour of nanostructured ZSM-5 catalysts prepared via ultrasound assisted rapid hydrothermal design was tested in MTP reaction.

2. Experimental

2.1. Chemicals

For ZSM-5 synthesis, fumid silica (Aldrich, 99.8%), sodium aluminate (Riedel-deltane Haën, 99%), sodium hydroxide (Merck, 97%) and tetra-propylammonium bromide (TPABr, Merck, 99.9%) were used as the sources of Si, Al, Na and template, respectively. The ion-exchange of Na^+ with H^+ was carried out using ammonium nitrate solution (Merck, 99%). It should be noted that deionized water was purchased from Kasra Company and employed in this experiment.

2.2. Preparation

The ZSM-5 nanostructured zeolites which prepared via conventional high temperature hydrothermal method were prepared according to our pervious study [13,29]. The hydrothermal technique consists of different stages which are carried out sequentially. First, the amorphous precursors are mixed together with water plus at room temperature. The amorphous gel is then left to age for period of time at room temperature. This aging time is crucial in the synthesis of MFI materials and also has significant influence on the nucleation mechanism. Thereafter, the hydrothermal crystallization of the aged gel is done by heating at high temperature and short time. The hydrothermal crystallization leads to the secondary nucleation by aggregation of more nuclei, which followed by the crystal growth. In the next step, the post treatment approaches, like drying and calcination, provide the more practical route to modify the prepared zeolite to acquire desirable framework compositions. For generating the final structure of HZSM-5, ion-exchanged step is needed to remove the Na species from the framework. In the case of ZSM-5 materials synthesized via ultrasound-assisted approach, the preparation procedure was not different dramatically from conventional route, except for the ultrasound step. The application of ultrasound, before the hydrothermal condition, can serve as an efficient step to enhance the crystallization mechanism.

In a typical synthesis as shown in Fig. 1S in supplementary material, the proper amount of sodium aluminate was added into a solution mixture of deionized water and sodium hydroxide. Then, TPABr as structure directing agent was added and mixed well at ambient temperature for 1 h. Finally, fumid silica was slowly added to the mixture and the produced gel aged under stirring for 24 h. In particular, for materials prepared by ultrasound-assisted method, the prepared gel was irradiated by sonication for 45 min at 90 W. An experimental setup for sonication treatment was applied (Ultrasonic Homogenizer, Ultrasonic Technology Development Co., Iran). The produced gel with molar ratio of $0.0025Al_2O_3{:}1SiO_2{:}0.1Na_2O$: $0.1TPABr{:}35H_2O$ was poured in a 90 mL stainless-steel autoclave and crystallized at high temperature synthesis condition (Table 1). The crystallization process was carried out at 250 °C for 3 h and 300 °C for 1.5 h in accordance with our previous studies and on the base of the crystalline phase nature. The resulting solid was recovered by filtration and washed several times with deionized water and then dried in air ambient at 110 °C for 12 h. The dried powder was calcined at 550 °C for 15 h. Finally, the ion-exchange process was applied to convert the NaZSM-5 solid powder to the HZSM-5. For this purpose, ammonium nitrate solution (1 mol/L) was used at 80 °C with reflux for 12 h and followed by filtration, washing and drying at 110 °C for 12 h. This ion displacement process was done for two times to obtain HZSM-5 zeolite. The final material was calcined under air flow at 500 °C for 4 h. These materials were designated as CH-x and UH-x where x was the crystallization temperature (x = 250 and 300 °C) and also CH and UH referred to conventional high temperature hydrothermal method and ultrasound-assisted high temperature hydrothermal method, respectively. Accordingly, the hydrothermal temperature (250 and 300 °C), crystallization time (3 and 1.5 h) and also synthesis approach (with and without ultrasound) are the main variables for preparation of MFI materials. In the following sections, the changes in these variables and their influences on the characterization results and also catalytic performances will be reviewed.

2.3. Characterization

The crystallinity and phase composition of all prepared samples were

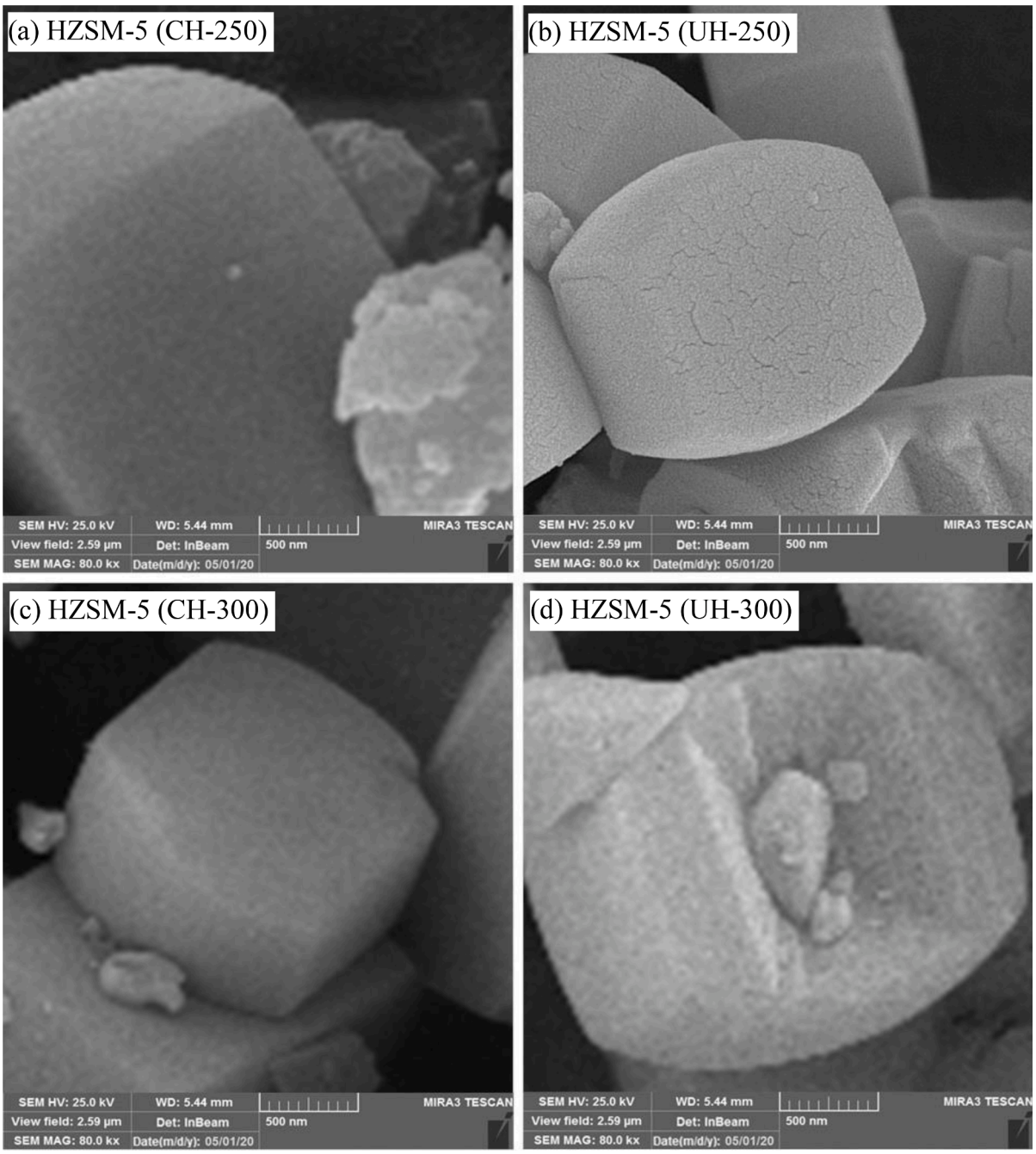

Fig. 2. FESEM images of efficient nanostructured MFI-type aluminosilicate catalysts: (a) HZSM-5 (CH-250), (b) HZSM-5 (UH-250), (c) HZSM-5 (CH-300) and (d) HZSM-5 (UH-300).

examined by means of X-ray diffraction measurement (XRD, Bruker D8 Advance diffractometer) by using Cu Kα radiation between $2\theta = 5^{\circ}$ and 55°. The field emission scanning electron microscopy (FESEM) was employed for study the surface morphology and surface particle size distribution by using HITACHI S-4160 instrument. Investigation of specific surface area, pore volume and pore diameter based on N_2 adsorption–desorption data by BET-BJH method were determined using Micrometrics ASAP 2020. The Fourier transform infrared (FTIR) spectra were performed to study the formation of chemical bonds by UNICAM 4600 FTIR spectroscopy. Moreover, the density and strength of acid sites in MFI zeolites were obtained using ammonia-temperature programmed desorption (TPD-NH_3) analysis and with a TPD/TPR 2900 analyzer. The measurement of TPD was started by heating in a stream of helium with a temperature program (rate of 15 °C min^{-1} up to 500 °C). After cooling the sample to 50 °C, ammonia flow was introduced to substitute helium for 10 min. The ammonia flow was then switched to helium flow for 30 min due to purge sample. Finally, the temperature was raised to 800 °C at a heating rate of 10 °C min^{-1} in helium atmosphere. Also, the amount of adsorbed ammonia was measured by utilizing a thermal conductivity detector (TCD). To study the deactivation of used catalysts by coke formation, thermo-gravimetric analysis (TGA) was monitored by a NETZSCH TG 209 F1 machine with thermal treatment. The temperature of used catalysts was raised from atmosphere temperature to 800 °C with rate of 10 °C min^{-1} under air.

2.4. Catalytic performance test

The synthesized MFI zeolites were tested as catalysts in an

experimental setup for methanol to propylene reaction which is shown in Fig. 2S in supplementary material. In a typical synthesis, 0.4 g of the zeolite (size 1–2 mm) was placed into a fixed bed reactor (i.d. = 8 mm, L = 32 cm) between the quartz frits. The U-shape reactor was heated inside the electric furnace via a temperature controlled. Before the catalytic performance test, the crushed sample into the reactor was preheated at 500 °C for 1 h Ar flow, due to removing the adsorbed water and organic materials through the pores. For feed stream generation, Ar flow (as carrier gas) with rate of 70 mL/min was passed through the saturator evaporator, which contained the liquid mixture of methanol–water with volume ratio of 1:1, and carried the methanol to the reactor with a gaseous space velocity (GHSV) of 10500 $cm^3/g_{cat}.h$. It can be noted that the vapour pressure of water is negligible compared to that of the methanol phase. So, the larger concentration of methanol entered the reactor by Ar stream. Also, the saturator evaporator was held in the ice-bath with constant temperature of 15 °C; due to the methanol vapour pressure remained constant during the catalytic performance period. Finally, a gas chromatograph (GC Chrom, Teif Gostar Faraz, Iran) with flame ionization detector (FID) and Plot-U capillary column (Agilent) was used for analyzing the outlet effluent stream.

3. Results and discussions

3.1. Physicochemical characterizations

3.1.1. XRD analysis

The XRD results of the prepared zeolites are depicted in Fig. 1. Two different phases of SiO_2 and ZSM-5 can be observed for the synthesized materials, which correspond to the high temperature synthetic conditions and our previous research results [29,39]. Comparison of these phases for samples indicates that the tetragonal structure of ZSM-5 and hexagonal phase of SiO_2 are observed in different ratios. Characteristic diffraction peaks at $2\theta = 7.9, 8.9, 9.1, 14.9, 20.9$, and 23.2° are related to the presence of ZSM-5 phase with MFI structure (JCPDS No. 00–044-0002) for all HZSM-5 (CH-250), HZSM-5 (UH-250), HZSM-5 (CH-300) and HZSM-5 (UH-300) catalysts [10,13]. Furthermore, the formation of SiO_2 impurity phase (JCPDS No. 01–085-0794) for HZSM-5 (CH-250), HZSM-5(CH-300) and HZSM-5 (UH-300) samples is confirmed by diffraction peaks centered at $2\theta = 20.9, 26.7, 36.7, 39.6, 42.6$ and 50.3° [29,40]. It is evident that the pure ZSM-5 framework is fully crystallized for HZSM-5 (UH-250) sample. It is strongly suggested the appearance of an appropriate number of nuclei during the gel aging and also greatly accelerating of crystallization process by non-spontaneous nucleation within sonication. So, ultrasound irradiation causes the stable supersaturation that leads to the formation of large number of uniform nuclei (primary nucleation) for HZSM-5 (UH-250) in comparison with the HZSM-5 (CH-250). In the presence of ultrasound treatment, the crystallization time of 3 h is sufficient enough to growth the large number of germ nuclei, which created in the ultrasonic assisted aging, to a certain critical sizes followed by secondary nucleation and as well as crystal growth. So, there is no extended crystallization time due to metastable phase transition which occurs and is converted into the secondary amorphous phase. On the other hand, the low primary nucleation density of HZSM-5 (CH-250), in the aging treatment without ultrasound assisted, leads to the rapid formation of aluminosilicate crystalline linkages during the crystallization process. This is the reason why the unstable MFI phase begins to transform into thermodynamically stable SiO_2 phase under the conventional hydrothermal condition

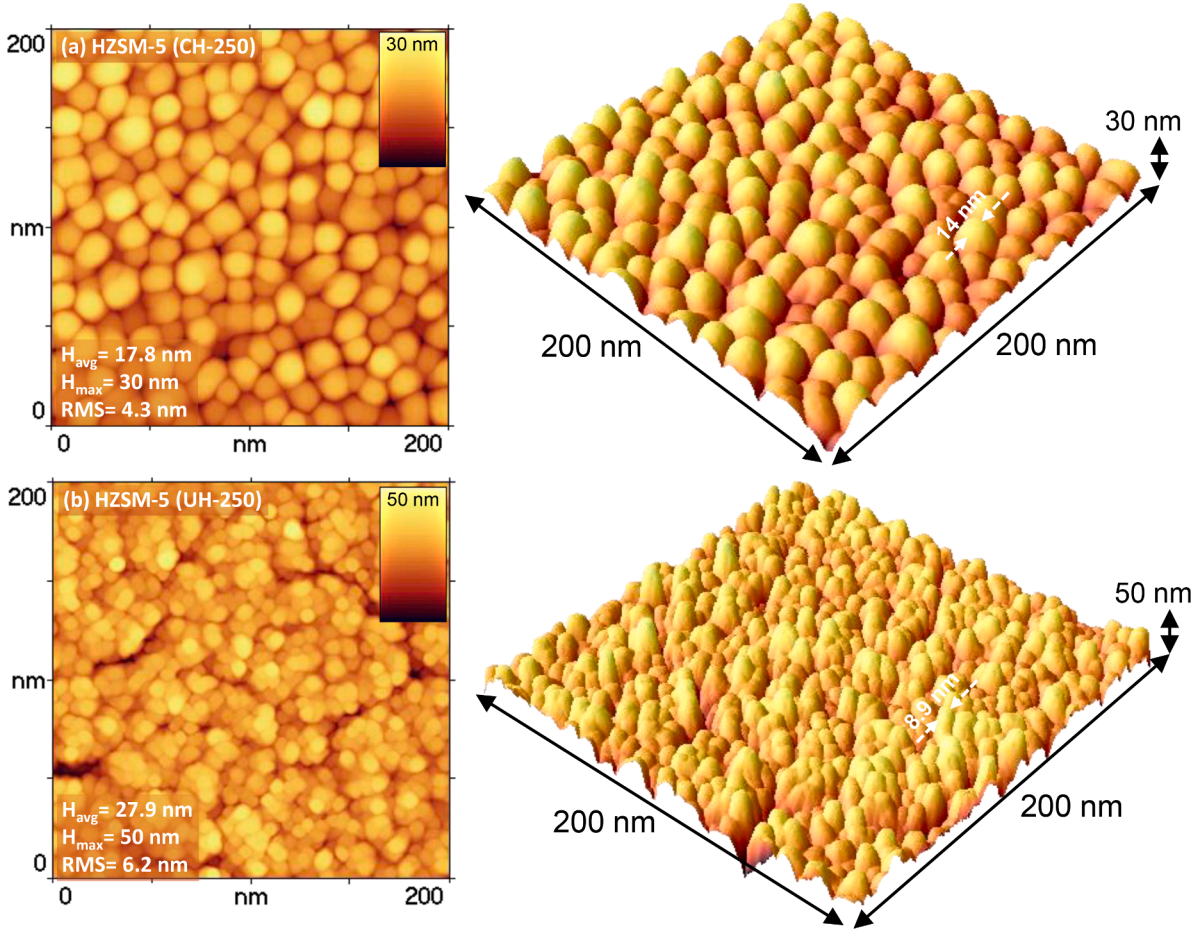

Fig. 3. Overview of 3D surface images of efficient nanostructured MFI-type aluminosilicate catalysts: (a) HZSM-5 (CH-250) and (b) HZSM-5 (UH-250).

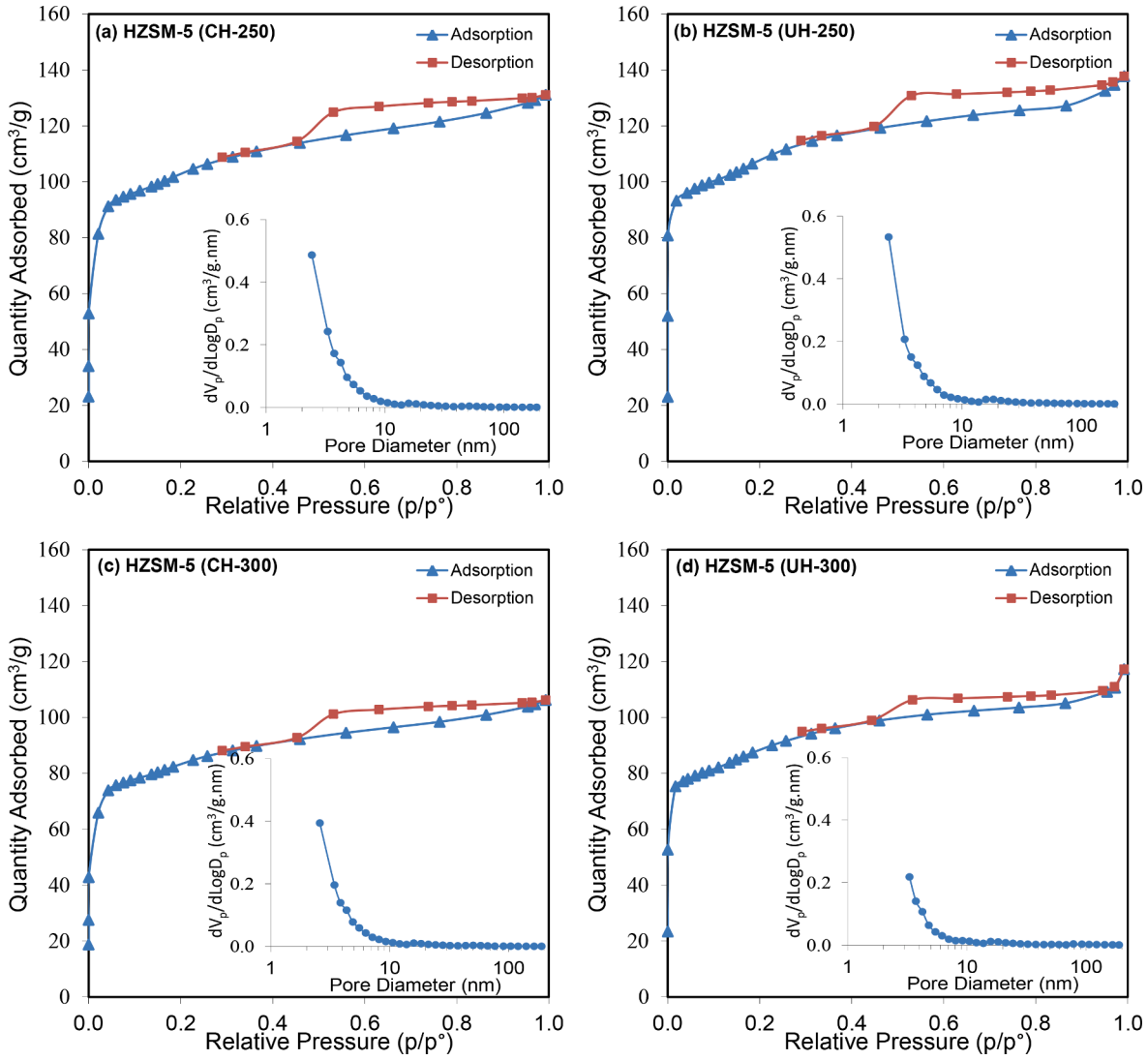

Fig. 4. Adsorption/Desorption isotherms and pore size distribution of efficient nanostructured MFI-type aluminosilicate catalysts: (a) HZSM-5 (CH-250), (b) HZSM-5 (UH-250), (c) HZSM-5 (CH-300) and (d) HZSM-5 (UH-300).

(250 °C and 3 h).

The synthesis factors can be affected by variation of crystallization temperature. So, different pore structures from a single synthetic system results in the formation of zeolites, due to the formation, dissolution and transformation of the gel. This suggests the nucleation and crystal growth and also the phase transition from metastable phase to stable phase [41]. By increasing the crystallization temperature to 300 °C, at crystallization time of 1.5 h, aluminosilicate ZSM-5 phase is observed with small amount of SiO_2 amorphous structure, when using the conventional high temperature hydrothermal method. A raise in crystallization temperature without ultrasound treatment causes a slight increase in the crystals growth rate and begins to produce an additional phase along with MFI framework. Furthermore, application of ultrasound irradiation assisted high temperature hydrothermal condition (300 °C and 1.5 h) favors the migration of ZSM-5 crystals leading to high amount of impurity SiO_2 phase. The change in the structure of the crystalline phase of HZSM-5 (UH-300) occurs via changes in the silicate species in the MFI crystalline framework. The result implies that higher temperature along with the sonochemical method is particularly effective for rapid secondary nucleation as well as enhancement of crystal growth, thereby causing the quick release of silicate species from the aluminosilicate framework to aggregate into large SiO_2 units during the crystallization time of 1.5 h.

It can be concluded that the peak intensities are shown the crystallinity of synthesized molecular sieves. Depending on the various crystallization conditions, it can be noted that the two main phases for each zeolite possess the different intensities and also different crystallinity in comparison with the other samples. According to enlarged peaks which are depicted above the Fig. 1, the intensity of characteristic peaks of ZSM-5 at $2\theta = 7.9$ and 8.9° related to (101) and (200) crystal facets increases with using ultrasound assisted moderate temperature and in contrast the growth of (112) crystal facet situated at $2\theta = 50.3^{\circ}$ belonged to SiO_2 phase decreases while the counterpart MFI phase increases. The growth rate of each facet varies with growth temperature gradient, synthesis time and ultrasonic treatment. The relative crystallinity of the synthesized structures based on the XRD relative peak intensity for HZSM-5 (UH-300), as reference sample, is depicted in Table 1. The relative crystallinity of MFI phase in HZSM-5 (CH-250), HZSM-5 (UH-250), HZSM-5 (CH-300) and HZSM-5 (UH-300) products is about 52.3%, 97.2%, 57.6% and 100%, respectively. Moreover, the relative crystallinity of SiO_2 phase for these materials is found to be 57.1%, 0.0%, 7.1% and 100%, respectively. However, ultrasound assisted high temperature of 300 °C simultaneously promotes the crystallinity of two competing phases of ZSM-5 and SiO_2. It should be noted that utilization of sonochemical method along with crystallization temperature of 250 °C is particularly useful only for the production of

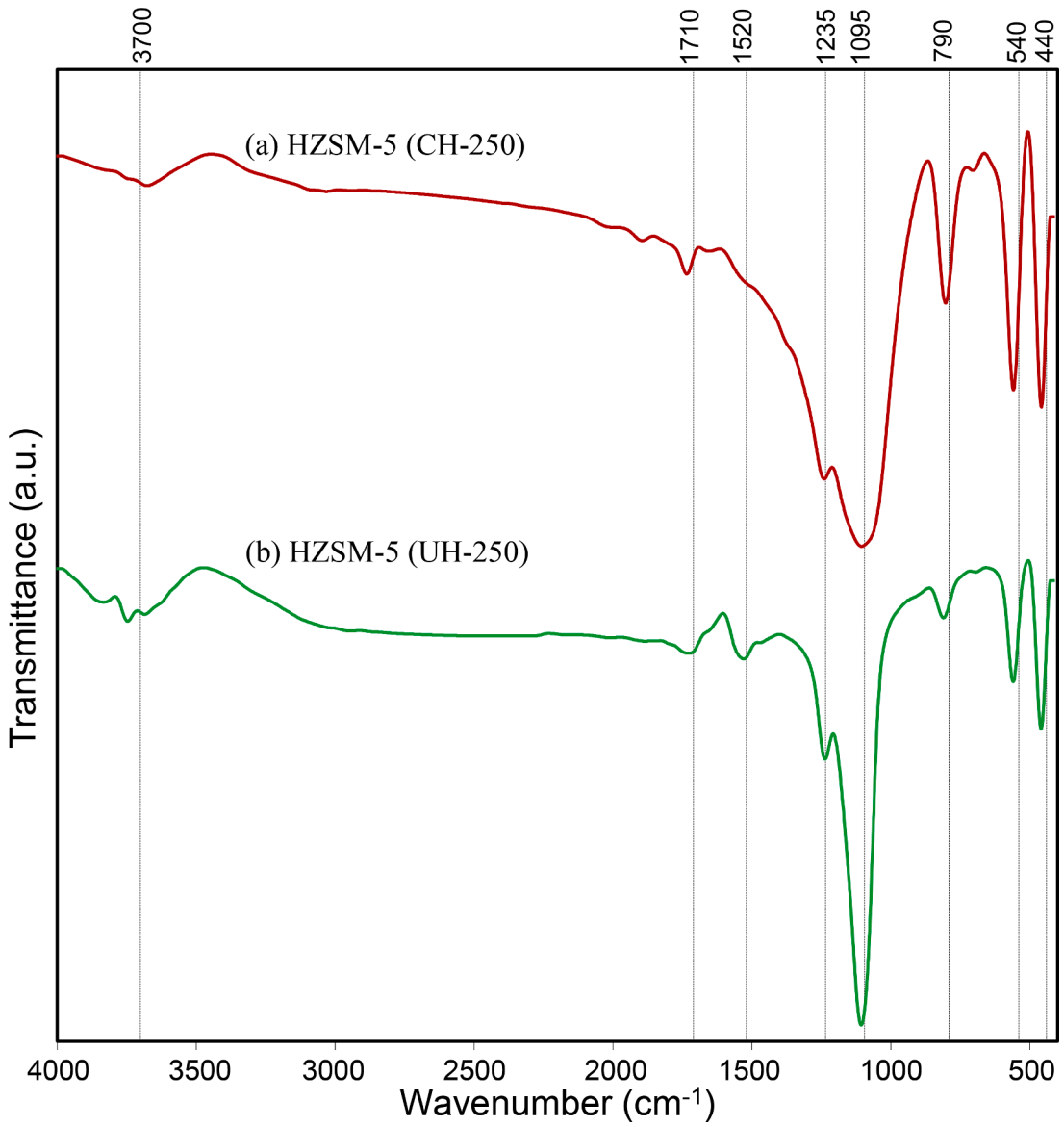

Fig. 5. FTIR spectra of efficient nanostructured MFI-type aluminosilicate catalysts: (a) HZSM-5 (CH-250) and (b) HZSM-5 (UH-250).

MFI crystalline structure. These observations support the above-mentioned explanation of the associated effects of ultrasound irradiation and high temperature synthesis to have a significant impact on the crystallization procedure.

3.1.2. Morphological analysis

The surface morphology and particle size distribution of prepared samples are analyzed by FESEM technique. As presented in Fig. 2, the ultrasound assisted hydrothermal method has not great effect on the morphology of MFI frameworks. The images of all samples indicate the coffin shape of HZSM-5 particles which are similar to that found in the literature [13,42]. As can be seen, the secondary amorphous phase of SiO_2 is deposited on the external surface of the MFI coffin particles of catalysts, except for the HZSM-5 (UH-250). With this deposition, the local adsorption at the entrance of pores and also the uptake rate into the MFI zeolites may be decreased. These results are in excellent agreement with the patterns of pervious XRD data. By using ultrasound assisted moderate temperature hydrothermal synthesis method (250 °C), relatively smaller ZSM-5 particles without SiO_2 agglomeration are formed. That could be due to an increase of nucleation rate and also a decrease of crystal growth rate during the crystallization process. It is clearly indicated that there is the largest particles for HZSM-5 (CH-250) catalyst synthesized without ultrasound irradiation.

Fig. 3 shows 3D surface images of nanostructured HZSM-5 (CH-250) and HZSM-5 (UH-250) aluminosilicate zeolites that were employed to investigate the roughness and surface topography. It can be seen that the height distribution for the two zeolites is asymmetrical, and the surfaces are formed by some peaks and valleys. However, the peaks are predominated in the surface morphology of catalysts, but HZSM-5 (UH-250) has more peaks than HZSM-5 (CH-250) zeolite. The root mean square roughness (RMS) represents the height variations, which this parameter is 4.3 and 6.2 nm for HZSM-5 (CH-250) and HZSM-5 (UH-250) samples, respectively. Also, the deviations in height are presented by the average surface height and are about 17.8 and 27.9 nm, respectively. According to the obtained results, ultrasound assisted rapid hydrothermal design of HZSM-5 (UH-250) zeolite increases the surface roughness, due to the perfect crystallization process. It is noted that the active sites interior of the crystalline system are fully accessible for molecules and has a significant beneficial effect in MTP catalytic reaction.

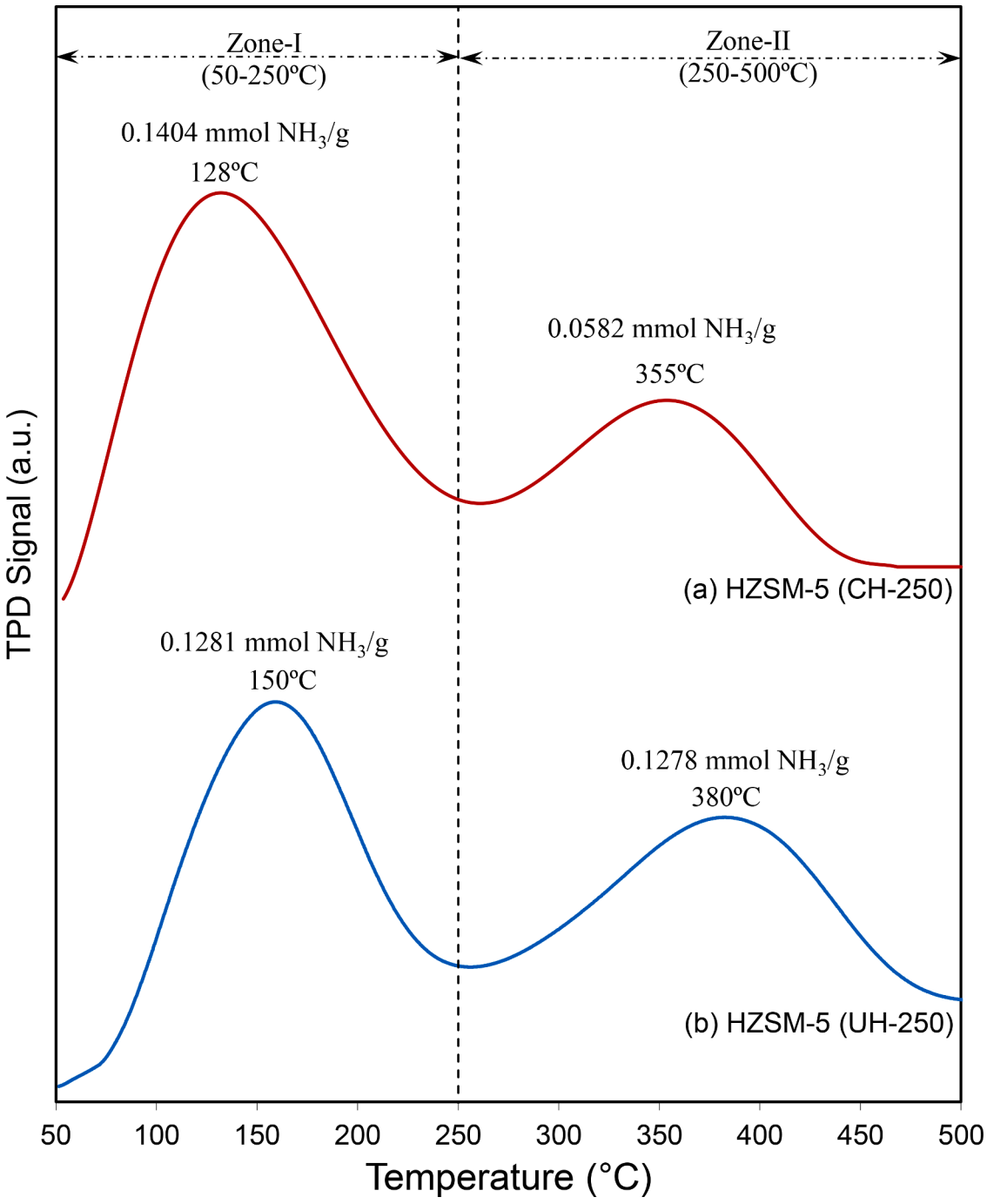

Fig. 6. TPD-NH_3 analysis of efficient nanostructured MFI-type aluminosilicate catalysts: (a) HZSM-5 (CH-250) and (b) HZSM-5 (UH-250).

3.1.3. BET-BJH analysis

N_2 adsorption/desorption isotherms and pore size distribution for all materials are demonstrated in Fig. 4. Regarding the IUPAC classification, the isotherms of catalysts are classified as the type-I, indicating the formation of microporous structure [13,39]. In addition, the mesopore size distribution of catalysts is plotted in Fig. 4, resulting from the BJH method. As shown, HZSM-5 catalysts synthesized with and without ultrasound assisted hydrothermal method exhibit the same mesopore size with diameters between 2 and 10 nm. On the other hand, this observation indicates that the sonochemical assisted moderate temperature of 250 °C results the high number of mesopores, which can be attributed to the complete crystallization of MFI framework with no amorphous phase that can collapse the pore structure. The detailed textural data for prepared zeolites, specific surface area and total pore volume, are presented in Table 1. The specific surface area of HZSM-5 (CH-250), HZSM-5 (UH-250), HZSM-5 (CH-300) and HZSM-5 (UH-300) samples are about 384, 397, 311 and 322 m^2/g, respectively. It is clearly seen that the HZSM-5 (UH-250) sample has the highest surface area (397 m^2/g) and also total pore volume (0.2024 cm^3/g) compared with the other catalysts. The production of SiO_2 dense phase along with MFI framework and as well as filling the HZSM-5 pores by silicate species can be the reason of this phenomenon, that can be confirmed by XRD and FESEM results. Surprisingly, it is found that the HZSM-5 (UH-300) catalyst has increased pore volume of about 0.1804 cm^3/g compared to the HZSM-5 (CH-300) zeolite, because it is referred to the high growing facets of MFI crystals along with the high degree of SiO_2 crystallinity resulted by using

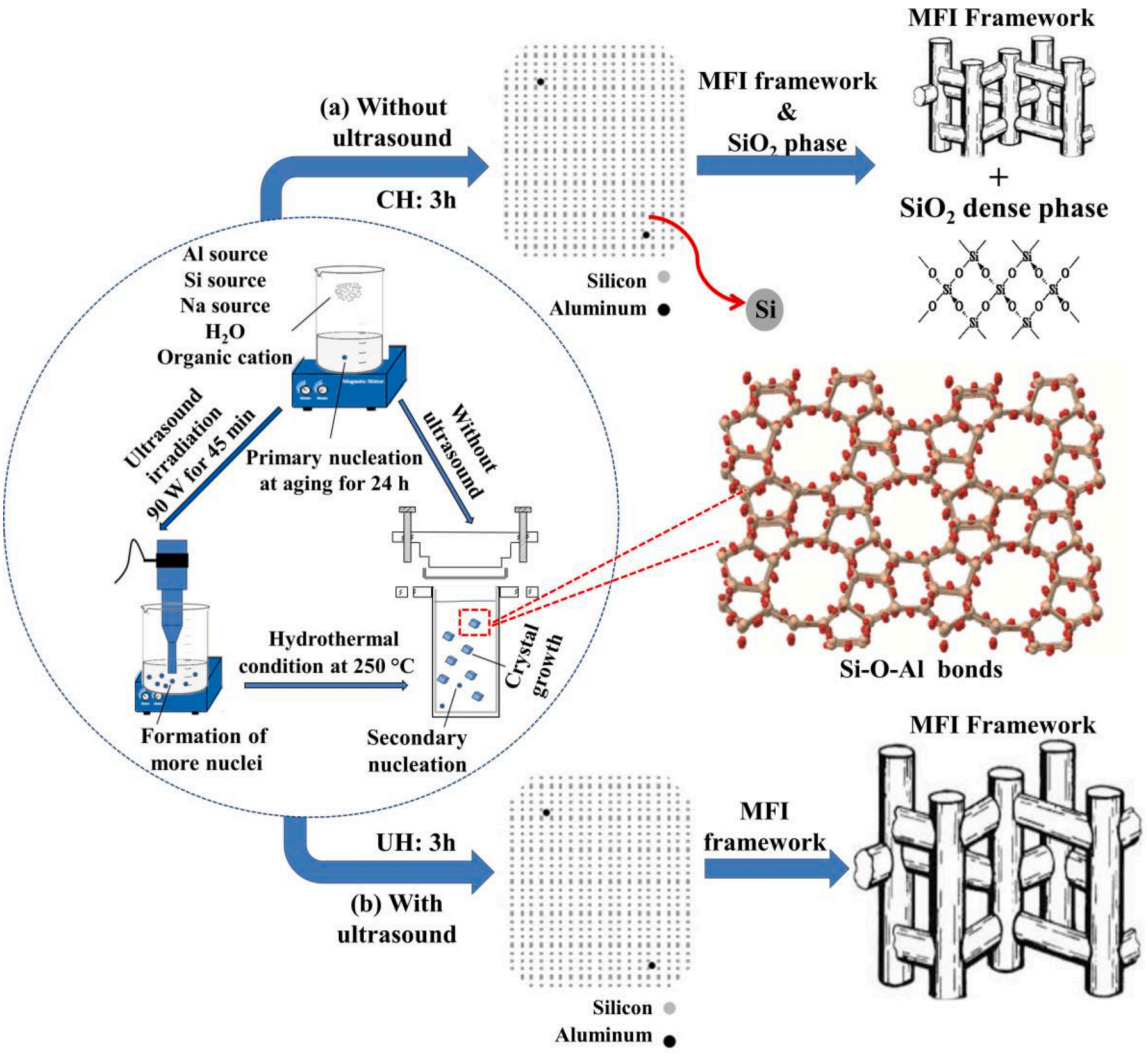

Fig. 7. Influence of ultrasound irradiation on synthesis pathway of efficient nanostructured MFI-type aluminosilicate catalyst.

ultrasound and high temperature synthesis approaches. According to the obtained results, a further catalytic activity enhancement for HZSM-5 (UH-250) catalyst is expected during the MTP reaction.

3.1.4. FTIR analysis

Fig. 5 shows FT-IR spectrums of HZSM-5 (CH-250) and HZSM-5 (UH-250) samples in the range of 500 and 4000 cm^{-1}. From the literature survey, the recorded peaks correspond to the MFI zeolite structure [29,43]. The observed peaks around 440 and 540 cm^{-1} are related to SiO_4 bending vibration and 5-membered rings, respectively [6]. Also, absorption bands at the range of 790 to 1520 cm^{-1} correspond to TO_4 tetrahedral and symmetric TOT modes [44]. It is indicative that the physically adsorbed water trapped inside cavities is contributed by the IR band at wavenumber about 1710 cm^{-1} [13,43]. Moreover, the characteristic peak in the wavenumber of 3700 cm^{-1} is related to the vibration hydroxyl groups, as active sites, that present in the ZSM-5 cage accessible in the straight ten-ring channel that involved change by applying ultrasound-assisted hydrothermal methods [6,29]. A more detailed description of these acid sites can be found in the subsequent characterization results.

3.1.5. TPD-NH_3 analysis

TPD curves for the characterization of the acid sites of HZSM-5 (CH-250) and HZSM-5 (UH-250) materials are shown in Fig. 6. For these zeolites, two kinds of desorption peaks are detected at temperature ranges of 50 to 250 °C and 250 to 500 °C, which are related to weak and strong active sites, respectively. The values in above of each peak are the density of acid sites calculated based on the areas under the each desorption peaks. The weak acid sites, that can be responsible for catalyzing the methanol-to-DME reaction, result from the coordinatively unsaturated cations and may also act as Lewis acid sites [7,10]. Furthermore, the strong active sites are related to the Brønsted acidic bridging protons on the framework that associated with silicon islands, leading to the formation of hydrocarbons from DME [23,42]. Comparing with HZSM-5(CH-250), HZSM-5 (UH-250) sample generates stronger acid site strength in the zeolitic structure. Furthermore, it is clearly indicated that the ultrasound assisted hydrothermal synthesis increases the concentration of strong active sites and decreases the density of weak acid sites. In this manner, due to increasing both the concentration and strength of ZSM-5 material, it is particularly desirable for introducing as much silicon into the MFI crystalline framework. The high electronegativity of silicon leads to the formation of Si sites with stronger acid site strength. Also, silicon atoms located out of the zeolite framework, as SiO_2 dense phase, produce no acid sites like the absence of active sites in a pure-silica zeolite. As a result, the presence of SiO_2 species out of the MFI framework that can be detected by pervious analyses causes the formation of weak acid sites for HZSM-5(CH-250) zeolite synthesized without ultrasound irradiation. Therefore, these amorphous materials can be prohibitive for advance in complete conversion of DME to light olefins process during the MTP reaction.

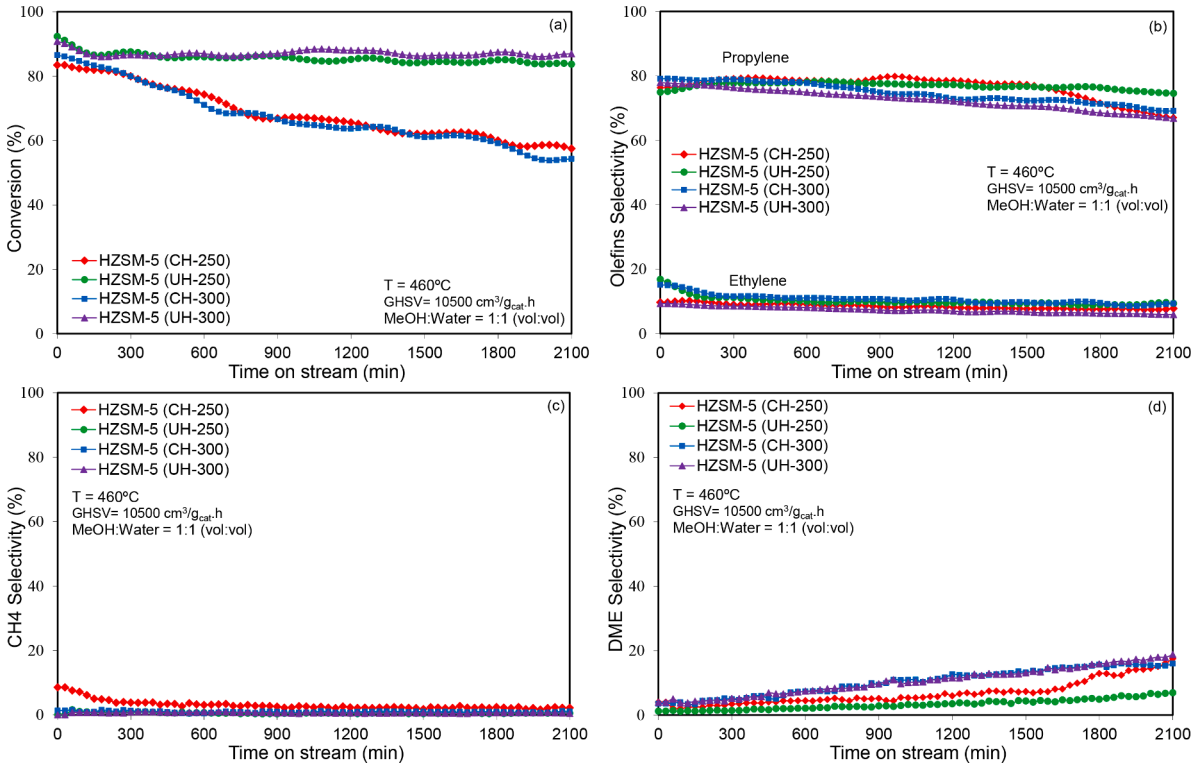

Fig. 8. Catalytic performance test over nanostructured MFI-type aluminosilicate catalysts: (a) methanol conversion, (b) olefins selectivity, (c) CH_4 selectivity and (d) DME selectivity.

3.2. *Influence of ultrasound on synthesis pathway of catalysts*

Fig. 7 depicts the influence of ultrasound irradiation on synthesis pathway of nanostructured MFI-type catalysts. In general, the resulting primary aluminosilicate gel is aged at ambient temperature, which usually results in affecting the nucleation process. In this step, the transformation of an initially amorphous intermediate species into a crystalline structure causes the formation of primary nucleation centers. Because of the accelerating of mass transfer by the collapse of cavitation bubbles in the mixture, application of ultrasound irradiation is favorable to produce the large number of nuclei. Therefore, prior to crystallization, the high density of growth nuclei presents for nanostructured zeolite synthesized via ultrasound-assisted hydrothermal method. Then, the crystallization process activated thermally due to control the production of the higher the yield of crystals at elevated temperature during 3 h period of time. In this manner, secondary nucleation begins uniformly when nucleation is induced by the formation of the same type of crystals. After a certain numbers of nuclei form and grow to observable size, the crystal growth takes place during the heating. The zeolite framework crystallized from this system is built up from Si-O-Al linkages with Si and Al vertices during the induction period. An increase in the crystal growth takes place under prolonging the crystallization time. Thus, the facets of MFI crystals begin to grow during the time. The more crystal nuclei of zeolite synthesized with ultrasound treatment is needed to larger crystallization time to organize complete ZSM-5 crystals without any framework defects. With ultrasound treatment, the crystallization time of 3 h is sufficient enough to growth the high density of nuclei, followed by secondary nucleation and as well as crystal growth. So, there is no extended crystallization time for transition of metastable phase to another secondary amorphous phase. In contrast, the faster growth of MFI crystals, with low number of nuclei, for catalyst synthesized via conventional hydrothermal method results in the formation of SiO_2 dense phase along with MFI structure, which can be generated from dislodged framework silicon species during the crystallization time. This proposed assembly pathway is in accordance with the characterization data of XRD and FESEM techniques.

3.3. *Catalytic performance study toward methanol to propylene*

3.3.1. *Effect of catalyst on methanol conversion and products selectivity*

Methanol conversion of synthesized aluminosilicate nanostructured catalysts with respect to time is presented in Fig. 8(a). The methanol conversion is defined as the following formula:

$$\text{Methanol conversion } (\%) = \frac{(\text{Initial methanol molar flow}) - (\text{Final methanol molar flow})}{(\text{Initial methanol molar flow})} \times 100$$

In the beginning of the reaction, the overall conversion level of all prepared materials is up to 80–85%. Furthermore, the conversion of methanol for HZSM-5(CH-250) and HZSM-5 (CH-300) materials continuously decreases with reaction time and reaches values blow about 60%. However, the conversion of zeolites synthesized with ultrasound irradiation assisted hydrothermal conditions is almost constant after 2100 min period of time. It can be observed that the ZSM-5(UH-250) and ZSM-5(UH-300) nanostructured catalysts with high growth of MFI crystals (Table 1) lead to the development of higher methanol conversion with prolonging the reaction time. Also, the fast blockage of

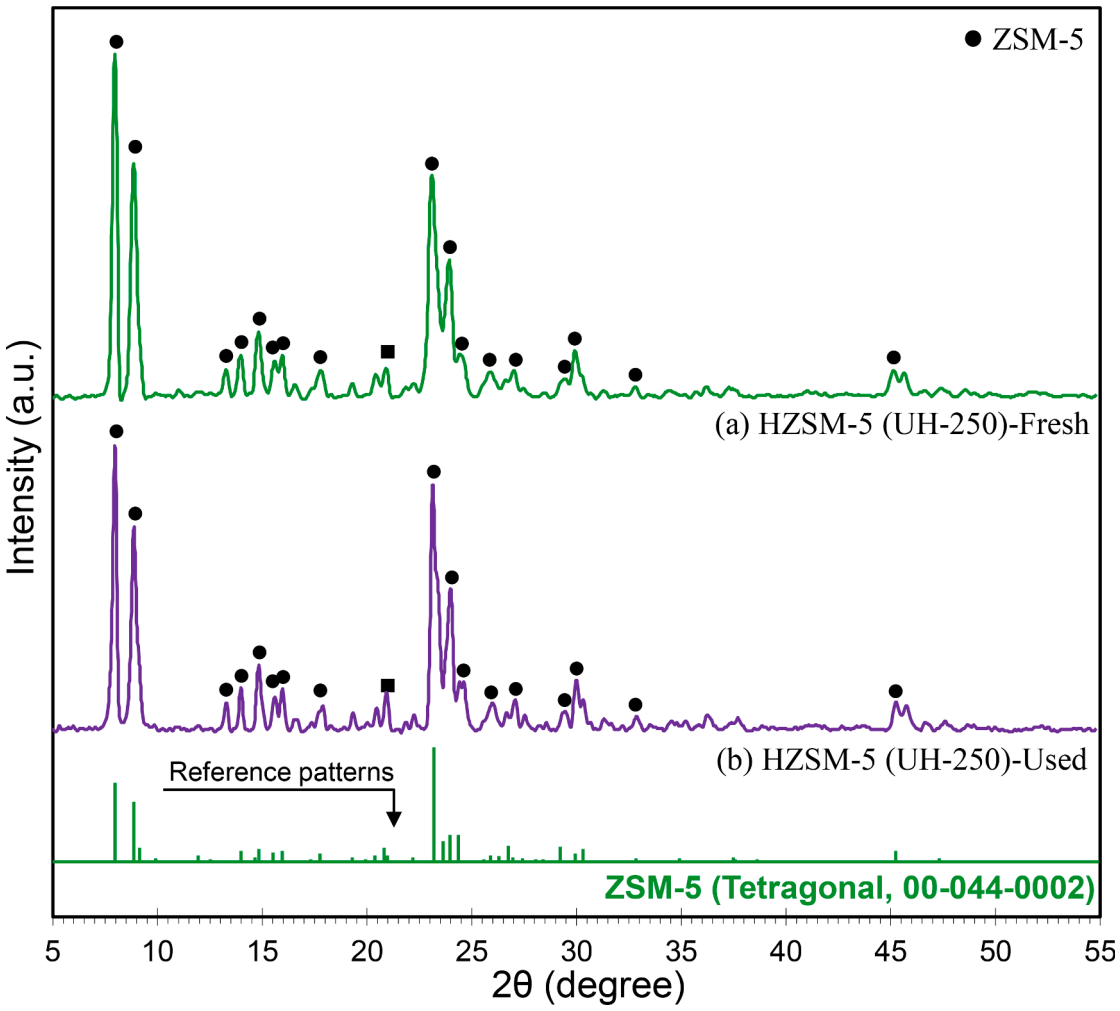

Fig. 9. XRD patterns of fresh and used HZSM-5 (UH-250) catalysts: (a) HZSM-5 (UH-250)-Fresh and (b) HZSM-5 (UH-250)-Used.

pore openings within HZSM-5(CH-250) and HZSM-5 (CH-300) crystals are responsible for reduction of methanol conversion during the time.

The products selectivity of synthesized catalysts is carried out under reaction condition (GHSV = 10500 $cm^3/g_{cat}.h$, T = 460 °C and CH_3OH: Water (vol:vol) = 1:1). In this regard, Fig. 8(b) shows the olefins selectivity over nanostructured MFI-type zeolites under 2100 min of time on stream (TOS). The product selectivity is calculated by the following equation:

$$\text{Product selectivity } (\%) = \frac{\text{Molar flow of specific product}}{\text{Total molar flow of all products}} \times 100$$

In view of ethylene, however, the initial ethylene selectivity is relatively higher for ZSM-5(UH-250) and ZSM-5(CH-300) catalysts. Nevertheless, it can be seen that the same ethylene selectivity (above 10%) is observed for all samples after 2100 min. By increasing the process time, propylene selectivity over HZSM-5(CH-250), HZSM-5(CH-300) and HZSM-5(UH-300) zeolites gradually decreases from initial value of 78 to 70%. In contrast, the initial value of propylene selectivity for HZSM-5(UH-250) material remains unchanged with prolonged time. In other words, the specific structural, textural, acidic and surface properties of HZSM-5(UH-250) zeolite cause to appear the constant olefins selectivity after extended periods of time. On the other hand, the presence of impurity SiO_2 phase along with MFI structure affects the selectivity of target products for other synthesized catalysts. Moreover, methane selectivity over nanostructured catalysts is depicted in Fig. 8 (c). The methane intermediate stands as a by-product for methanol to propylene process, which results from DME thermal decomposition reaction. According to the slower hydrogen transfer rate and higher resistance to deactivation, our synthesized zeolites have negligible amount of methane with time. On the other hand, Fig. 8(d) shows the DME selectivity for all MFI-type aluminosilicate zeolites. It can be observed that the DME production of samples increases with increasing reaction time. The low accessibility of active sites and subsequent blockage of zeolites pores that are connected with coke formation can lead to an increasing formation of DME product with time [45,46]. Furthermore, the minimum DME productivity (7%) is obtained for HZSM-5(UH-250) catalyst during the reaction period of 2100 min. As a result, the ultrasound-assisted moderate temperature synthesis route leads to the production of zeolite with superior in structural properties for the MTP application.

3.3.2. *Deactivation study*

Deactivation study of HZSM-5(UH-250) sample is investigated by XRD, TG/DTG and morphological analyses. In this way, Fig. 9 demonstrates the XRD patterns of fresh and used HZSM-5(UH-250) nanostructured catalyst. As can be seen, there is only a minor decline in the peaks intensity of used HZSM-5(UH-250) zeolite in comparison to the fresh sample. The outcomes indicate that the structure of MFI-type aluminosilicate HZSM-5(UH-250)-Used catalyst remains unchanged during the MTP reaction. This can be attributed to the low rate of coke deposition and its growth in corresponded of the unique structure of MFI porous material. For a detailed survey on the deactivation behaviour of HZSM-5(UH-250) catalyst, the TG/DTG analysis is carried out. Fig. 10 shows the TG/DTG results of nanostructured HZSM-5(CH-250)-Used

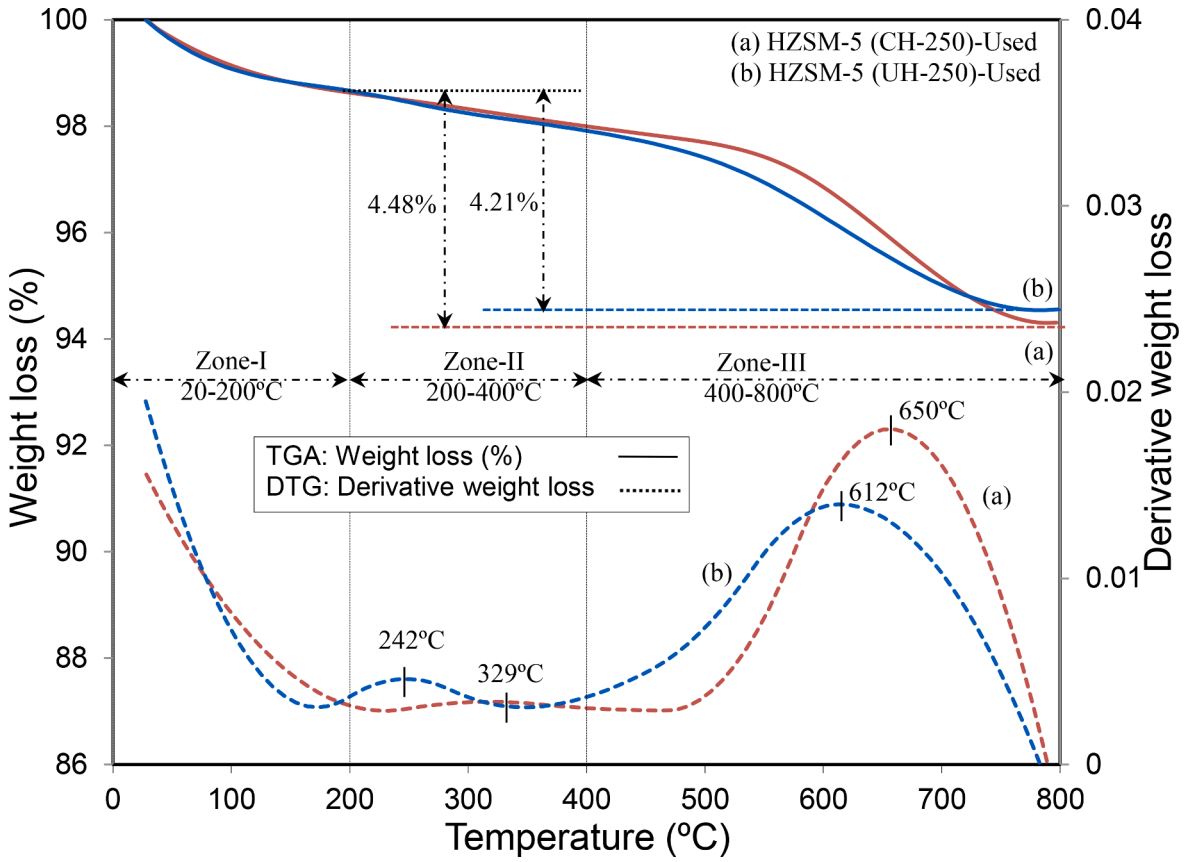

Fig. 10. TG/DTG analysis of used nanostructured MFI-type aluminosilicate catalysts: (a) HZSM-5 (CH-250)-Used and (b) HZSM-5 (UH-250)-Used.

and HZSM-5(UH-250)-Used catalysts. Three distinct groups of weight losses are observed in both zeolites: 20–200, 200–400 and 400–800 °C. The first weight loss can be associated to the release of moisture and physically adsorbed water [20]. In this zone, the low weight loss for both HZSM-5(CH-250) and HZSM-5(UH-250) catalysts can be attributed to the hydrophobic nature of MFI framework, which leads to the low adsorption capacity of water inside the pores. The other two losses correspond to the coke deposition on the surface of catalysts [38]. Moreover, the vast majority of weight loss is observed around 400 and 800 °C. This can be explained by the formation of the type of coke residual, which can be burnt off at higher temperatures. The coke deposition can cover the acid sites, block the pores, and gradually deactivate the catalyst during the methanol to propylene reaction. Accordingly, the total coke contents for HZSM-5(CH-250)-Used and HZSM-5(UH-250)-Used samples are about 4.48% and 4.21%, respectively. As a result, the low coke formation for HZSM-5(UH-250)-Used sample causes the slow deactivation rate of this zeolite that synthesized with ultrasound application. Based on the DTG curves, it can be concluded that the two kinds of carbonaceous materials, soft and hard cokes, are deposited on the surface of catalysts. The monoaromatic and polyaromatic compounds are responsible for the formation of carbonaceous species and as well as deactivation of catalyst. There are essential differences in the nature, distribution and quantity of these two coke species deposited in the MFI crystalline framework. These observations are supported by the peaks position and also their area, which allow the detection of coking propensity of synthesized zeolites. In this manner, peaks shift to lower temperature region for HZSM-5(UH-250)-Used catalyst, which means the formation of softer coke can be burnt off more easily. Thus, the HZSM-5(UH-250)-Used catalyst has softer coke than the HZSM-5(CH-250)-Used zeolite. Also, the high amount of cokes, especially the hard coke, is formed in the HZSM-5(CH-250)-Used zeolite. As a result, ultrasound-assisted for HZSM-5(UH-250) synthesis leads to produce an active molecular sieve within the well-defined geometry which prohibits the formation of monoaromatic and polyaromatic compounds during the steps of MTP reaction.

Also, Fig. 11 presents the morphological analysis of HZSM-5(UH-250)-Used nanostructured MFI-type aluminosilicate material. By comparing the morphological images of HZSM-5(UH-250)-Used catalyst with respect to the images of fresh HZSM-5(UH-250) sample (as in Fig. 2), it can be noted the formation of coke on the surface of the HZSM-5(UH-250)-Used particles. Furthermore, there is only a minor growth of coke on the surface of HZSM-5(UH-250)-Used sample. Accordingly, the low coke formation deposited during the 2100 min is effective for low rate of blocking the pore entrances which leads to the passage of the molecules that can access to the active sites.

From the results that obtained by deactivation study, the proposed deactivation mechanism of nanostructured HZSM-5(UH-250) catalyst is exhibited in Fig. 12. In a major route, 7 sequential steps of the catalytic reaction present at the porous structure of HZSM-5(UH-250) sample. These steps contain: 1) mass transfer of methanol to catalyst surface, 2) internal diffusion of methanol from pore entrance to catalytic surface, 3) methanol adsorption onto active sites of catalyst, 4) MTP process on the catalytic surface, 5) product desorption over the surface, 6) product diffusion from pellet interior to pore entrance and 7) product diffusion from external surface to the bulk. During the MTP process, methanol is first dehydrated to DME and water by adsorbing on the active sites of MFI-type aluminosilicate material. Subsequently, the resulting equilibrium between DME, methanol and water interact with the stronger acid sites and form the C–C bonds, especially propylene. With prolonging the reaction time, the produced materials can polymerize into ‘‘soft coke’’ via hydrogen transfer process. These carbonaceous species, which contain monoaromatic compounds, do not generally block the zeolite channels [47,48]. So, they are not responsible for immediate effect on the catalyst deactivation. Finally, the transformation of ‘‘ soft coke’’ to

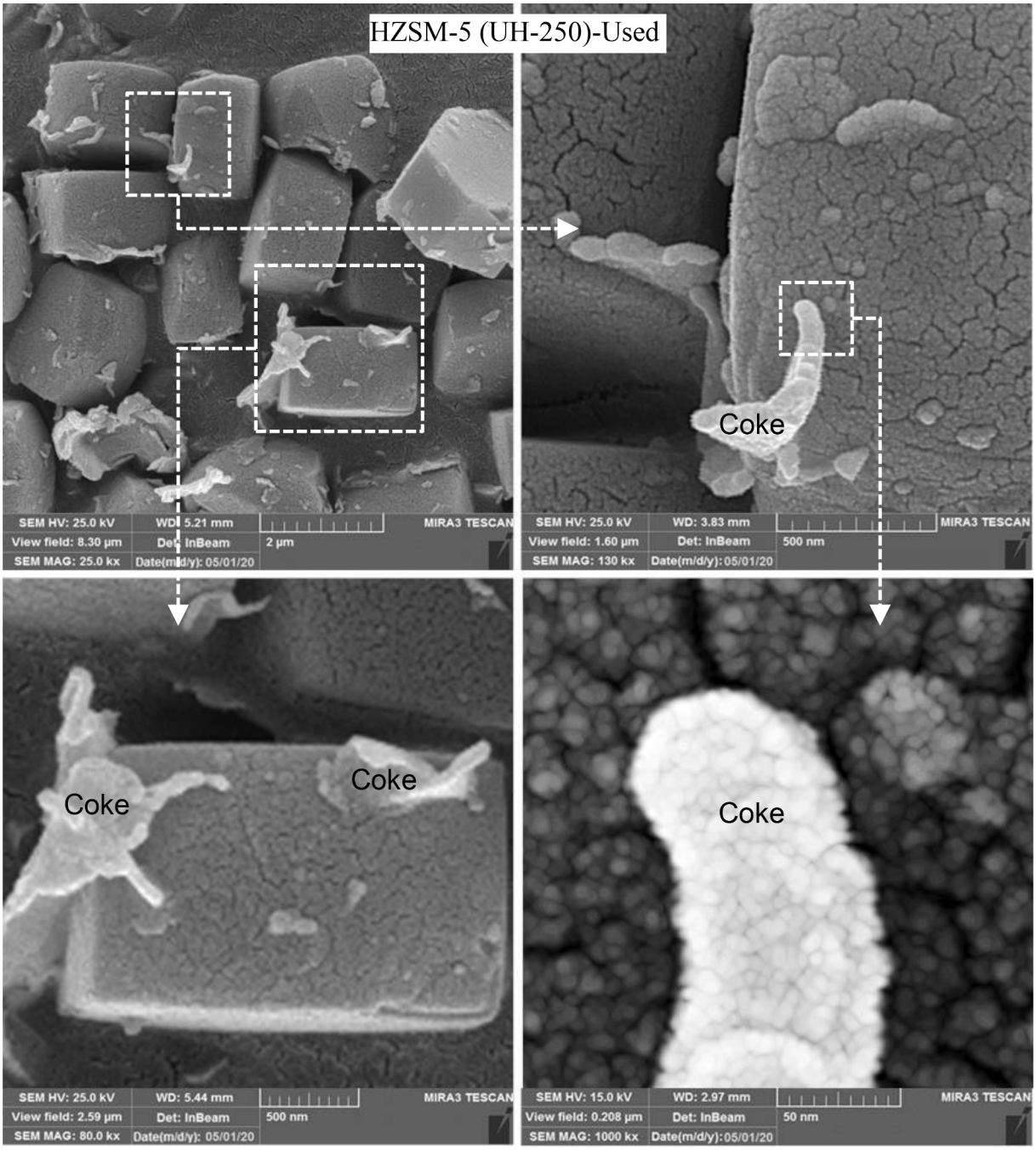

Fig. 11. Morphological analysis of used nanostructured MFI-type aluminosilicate catalyst: HZSM-5 (UH-250)-Used.

''hard coke'' takes place through condensation and hydrogen transfer during the long time on stream experiment. The growing of poly-aromatic compounds as '' hard coke'' relates to the crystalline structure and acidity of catalyst that lead to the deactivation and as well as activity decay by pore blocking [49]. These formed coke species which deposit on the external surface of coffin shape particles can lead to the blocking of pore mouth impeding the access to the acid sites in the crystalline structure. As a result, the HZSM-5(UH-250) molecular sieve synthesized with ultrasound-assisted possess the slower deactivation regime which makes it good candidate for application in the MTP catalytic process.

4. Conclusions

In this study, application of ultrasound irradiation before the rapid hydrothermal crystallization of MFI-type zeolites was studied, and the obtained results were compared with those of ZSM-5 materials synthesized without ultrasound approach. The obtained results indicated that ultrasound-assisted moderate temperature hydrothermal synthesis of MFI-type aluminosilicate framework had a positive influence on the structural features and physicochemical properties associated with enhanced performance in the MTP reaction. Accordingly, it was found that the HZSM-5(UH-250) sample showed the perfect crystallization process, leading to the formation of pure MFI phase with any structural crystal defects. Based on this fine crystalline structure, the surface roughness, pore volume and acidity concentration were increased.

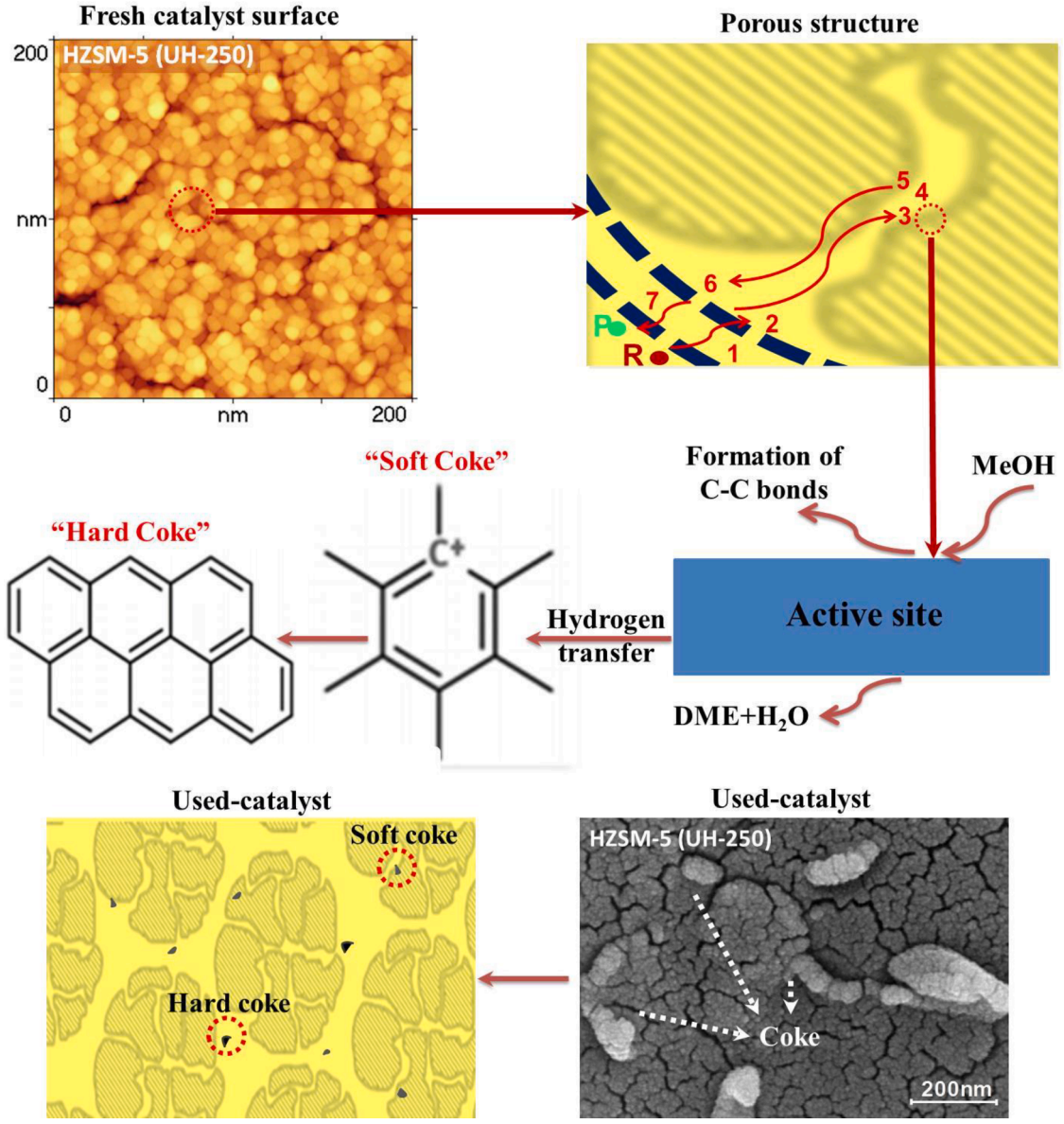

Fig. 12. Deactivation mechanism of nanostructured MFI-type aluminosilicate catalyst used in methanol to propylene reaction.

Consequently, the MTP catalytic performance of synthesized samples revealed that the existence of SiO_2 amorphous species along with MFI framework was prohibitive for advance in methanol conversion to propylene. In contrast, the prepared HZSM-5(UH-250) zeolite with low coke deposition led to the development of a promising catalyst, which provided the enhanced methanol conversion and significant propylene selectivity during the reaction time.

CRediT authorship contribution statement

Parisa Sadeghpour: Conceptualization, Methodology, Investigation, Writing - original draft. **Mohammad Haghighi:** Project administration, Conceptualization, Methodology, Resources, Visualization, Supervision, Writing - review & editing. **Alireza Ebrahimi:** Conceptualization, Methodology, Investigation, Writing - review & editing.

Declaration of Competing Interest

The authors declare that they have no known competing financial interests or personal relationships that could have appeared to influence the work reported in this paper.

Acknowledgement

The authors gratefully acknowledge Sahand University of Technology for the financial support of the research as well as Iran Nanotechnology Initiative Council for complementary financial supports.

Appendix A. Supplementary data

Supplementary data to this article can be found online at https://doi.org/10.1016/j.ultsonch.2020.105416.

References

[1] E. Aghaei, M. Haghighi, Z. Pazhohniya, S. Aghamohammadi, One-Pot Hydrothermal Synthesis of Nanostructured ZrAPSO-34 Powder: Effect of Zr-Loading on Physicochemical Properties and Catalytic Performance in Conversion of Methanol to Ethylene and Propylene, Microporous Mesoporous Mater. 226 (2016) 331–343.

[2] M.S. Ahmad, C.K. Cheng, P. Bhuyar, A.E. Atabani, A. Pugazhendhi, N.T.L. Chi, T. Witoon, J.W. Lim, J.C. Juan, Effect of reaction conditions on the lifetime of

SAPO-34 catalysts in methanol to olefins process – A review, Fuel 283 (2021), 118851.
[3] S. Standl, F.M. Kirchberger, T. Kühlewind, M. Tonigold, M. Sanchez-Sanchez, J. A. Lercher, O. Hinrichsen, Single-event kinetic model for methanol-to-olefins (MTO) over ZSM-5: Fundamental kinetics for the olefin co-feed reactivity, Chem. Eng. J. 402 (2020), 126023.
[4] S. Wang, Y. Chen, Z. Qin, T.-S. Zhao, S. Fan, M. Dong, J. Li, W. Fan, J. Wang, Origin and evolution of the initial hydrocarbon pool intermediates in the transition period for the conversion of methanol to olefins over H-ZSM-5 zeolite, J. Catal. 369 (2019) 382–395.
[5] A. Ebrahimi, M. Haghighi, S. Aghamohammadi, Effect of Calcination Temperature and Composition on the Spray-Dried Microencapsulated Nanostructured SAPO-34 with Kaolin for Methanol Conversion to ethylene and propylene in Fluidized Bed Reactor, Microporous Mesoporous Mater. 297 (2020), 110046.
[6] K. Khaledi, M. Haghighi, P. Sadeghpour, Influence of surface design on performance of MnO-decorated nanocatalyst for olefin production from methanol: ZSM-5@MnO core–shell versus MnO/ZSM-5 dispersed nanocatalysts, J. Chem. Technol. Biotechnol. 95 (2020) 2447–2462.
[7] M. Rostamizadeh, A. Taeb, Highly selective Me-ZSM-5 catalyst for methanol to propylene (MTP), J. Ind. Eng. Chem. 27 (2015) 297–306.
[8] S. Aghamohammadi, M. Haghighi, A. Ebrahimi, Fabrication of Attrition-Resistant Nanostructured Catalyst by Spray Dryer for Methanol to Light Olefins Reaction in a Fluid Bed Reactor and Coke Formation, Microporous Mesoporous Mater. 279 (2019) 371–386.
[9] R. Feng, X. Wang, J. Lin, Z. Li, K. Hou, X. Yan, X. Hu, Z. Yan, M.J. Rood, Two-stage glucose-assisted crystallization of ZSM-5 to improve methanol to propylene (MTP), Microporous Mesoporous Mater. 270 (2018) 57–66.
[10] P. Sadeghpour, M. Haghighi, M. Esmaeili, Structural/Texture Evolution During Facile Substitution of Ni into ZSM-5 Nanostructure vs. its Impregnation Dispersion Used in Selective Transformation of Methanol to Ethylene and Propylene, Combinatorial Chemistry & High Throughput Screening, (2020 (In Press)).
[11] Y. Xue, J. Li, P. Wang, X. Cui, H. Zheng, Y. Niu, M. Dong, Z. Qin, J. Wang, W. Fan, Regulating Al distribution of ZSM-5 by Sn incorporation for improving catalytic properties in methanol to olefins, Appl. Catal. B 280 (2021), 119391.
[12] M. Firoozi, M. Baghalha, M. Asadi, The effect of micro and nano particle sizes of H-ZSM-5 on the selectivity of MTP reaction, Catal. Commun. 10 (2009) 1582–1585.
[13] P. Sadeghpour, M. Haghighi, P. Shekari, Facile moderate-temperature hydrothermal design of nanocrystalline coffin-shaped ZSM-5 catalyst for transformation of CH3OH to C2H4/C3H6, Part. Sci. Technol. 38 (2020) 898–911.
[14] S. Sadeghi, M. Haghighi, P. Estifaee, Methanol to Clean Gasoline over Nanostructured CuO-ZnO/HZSM-5 Catalyst: Influence of Conventional and Ultrasound Assisted Co-impregnation Synthesis on Catalytic Properties and Performance, J. Nat. Gas Sci. Eng. 24 (2015) 302–310.
[15] Y. Zhang, M. Li, E. Xing, Y. Luo, X. Shu, Coke evolution on mesoporous ZSM-5 during methanol to propylene reaction, Catal. Commun. 119 (2019) 67–70.
[16] S. Allahyari, M. Haghighi, A. Ebadi, S. Hosseinzadeh, Ultrasound assisted co-precipitation of nanostructured CuO–ZnO–Al2O3 over HZSM-5: Effect of precursor and irradiation power on nanocatalyst properties and catalytic performance for direct syngas to DME, Ultrason. Sonochem. 21 (2014) 663–673.
[17] F. Rahmani, M. Haghighi, B. Mohammadkhani, Enhanced Dispersion of Cr Nanoparticles over Nanostructured ZrO2-Doped ZSM-5 Used in CO2-Oxydehydrogenation of Ethane, Microporous Mesoporous Mater. 242 (2017) 34–49.
[18] D.-K. Yu, M.-L. Fu, Y.-H. Yuan, Y.-B. Song, J.-Y. Chen, Y.-W. Fang, One-step synthesis of hierarchical-structured ZSM-5 zeolite, J. Fuel Chem. Technol. 44 (2016) 1363–1369.
[19] M.J. Azarhoosh, R. Halladj, S. Askari, A. Aghaeinejad-Meybodi, Performance analysis of ultrasound-assisted synthesized nano-hierarchical SAPO-34 catalyst in the methanol-to-lights-olefins process via artificial intelligence methods, Ultrason. Sonochem. 58 (2019), 104646.
[20] S. Aghamohammadi, M. Haghighi, A. Ebrahimi, Pathways in particle assembly by ultrasound-assisted spray-drying of kaolin/SAPO-34 as a fluidized bed catalyst for methanol to light olefins, Ultrason. Sonochem. 53 (2019) 237–251.
[21] F. Liu, X. Wang, F. Xu, Q. Lin, H. Pan, H. Wu, J. Cao, Fabrication and characterization of composites comprising (CHA)SAPO-34 with (MFI)ZSM-5 topologies and their catalytic performances on MTO reaction, Microporous Mesoporous Mater. 252 (2017) 197–206.
[22] J. Valecillos, E. Epelde, J. Albo, A.T. Aguayo, J. Bilbao, P. Castaño, Slowing down the deactivation of H-ZSM-5 zeolite catalyst in the methanol-to-olefin (MTO) reaction by P or Zn modifications, Catal. Today 348 (2020) 243–256.
[23] M.S. Beheshti, M. Behzad, J. Ahmadpour, H. Arabi, Modification of H-[B]-ZSM-5 zeolite for methanol to propylene (MTP) conversion: Investigation of extrusion and steaming treatments on physicochemical characteristics and catalytic performance, Microporous Mesoporous Mater. 291 (2020), 109699.
[24] H. Li, Y. Wang, C. Fan, C. Sun, X. Wang, C. Wang, X. Zhang, S. Wang, Facile synthesis of a superior MTP catalyst: Hierarchical micro-meso-macroporous ZSM-5 zeolites, Appl. Catal. A 551 (2018) 34–48.
[25] L. Han, Y. Ouyang, E. Xing, Y. Luo, Z. Da, Enhancing hydrothermal stability of framework Al in ZSM-5: from the view on the transformation between P and Al species by solid-state NMR spectroscopy, Chinese J. Chem. Eng., (2020 (In Press)).
[26] N. Kumar, O.V. Masloboischikova, L.M. Kustov, T. Heikkilä, T. Salmi, D.Y. Murzin, Synthesis of Pt modified ZSM-5 and beta zeolite catalysts: Influence of ultrasonic irradiation and preparation methods on physico-chemical and catalytic properties in pentane isomerization, Ultrason. Sonochem. 14 (2007) 122–130.
[27] H. Liu, S. Zhang, Y. Zhou, Y. Zhang, L. Bai, L. Huang, Effect of ultrasonic irradiation on the catalytic performance of PtSnNa/ZSM-5 catalyst for propane dehydrogenation, Ultrason. Sonochem. 18 (2011) 19–22.
[28] S. Vichaphund, V. Sricharoenchaikul, D. Atong, Selective aromatic formation from catalytic fast pyrolysis of Jatropha residues using ZSM-5 prepared by microwave-assisted synthesis, J. Anal. Appl. Pyrol. 141 (2019), 104628.
[29] P. Sadeghpour, M. Haghighi, High-temperature and short-time hydrothermal fabrication of nanostructured ZSM-5 catalyst with suitable pore geometry and strong intrinsic acidity used in methanol to light olefins conversion, Adv. Powder Technol. 29 (2018) 1175–1188.
[30] S.V. Sancheti, P.R. Gogate, A review of engineering aspects of intensification of chemical synthesis using ultrasound, Ultrason. Sonochem. 36 (2017) 527–543.
[31] T. Yit Siew Ng, T. Leng Chew, Y. Fong Yeong, Synthesis of small pore zeolite via ultrasonic-assisted hydrothermal synthesis, Mater. Today:. Proc. 16 (2019) 1935–1941.
[32] S. Zhuang, Z. Hu, L. Huang, F. Qin, Z. Huang, C. Sun, W. Shen, H. Xu, Synthesis of ZSM-5 catalysts with tunable mesoporosity by ultrasound-assisted method: A highly stable catalyst for methanol to propylene, Catal. Commun. 114 (2018) 28–32.
[33] E. Moradiyan, R. Halladj, S. Askari, Beneficial Use of Ultrasound in Rapid-Synthesis of SAPO34/ZSM-5 Nanocomposite and Its Catalytic Performances on MTO Reaction, Ind. Eng. Chem. Res. 57 (2018) 1871–1882.
[34] K. Parveen, U. Rafique, M. Javed Akhtar, M. Ashokkumar, Sonochemical synthesis of aluminium and aluminium hybrids for remediation of toxic metals, Ultrason. Sonochem. 70 (2021), 105299.
[35] H. Ramirez Mendoza, J. Jordens, M. Valdez Lancinha Pereira, C. Lutz, T. Van Gerven, Effects of ultrasonic irradiation on crystallization kinetics, morphological and structural properties of zeolite FAU, Ultrason. Sonochem. 64 (2020), 105010.
[36] F. Gorzin, J. Towfighi Darian, F. Yaripour, S.M. Mousavi, Synthesis of highly crystalline nanosized HZSM-5 catalyst employing combined hydrothermal and sonochemical method: Investigation of ultrasonic parameters on physico-chemical and catalytic performance in methanol to propylene reaction, J. Solid State Chem. 271 (2019) 8–22.
[37] A.A. Eslami, M. Haghighi, P. Sadeghpour, Short time microwave/seed-assisted synthesis and physicochemical characterization of nanostructured MnAPSO-34 catalyst used in methanol conversion to light olefins, Powder Technol. 310 (2017) 187–200.
[38] P. Sadeghpour, M. Haghighi, K. Khaledi, High-temperature efficient isomorphous substitution of boron into ZSM-5 nanostructure for selective and stable production of ethylene and propylene from methanol, Mater. Chem. Phys. 217 (2018) 133–150.
[39] R. Shokrani, M. Haghighi, Textural evolution of hierarchical nanostructured ZSM-5 via sono-hydrothermal design by various carbon shapes for efficient biodiesel production, Appl. Catal. B 271 (2020), 118940.
[40] S.T. Maung, T. Chanadee, S. Niyomwas, Two reactant systems for self-propagating high-temperature synthesis of tungsten silicide, J. Aust. Ceram. Soc. 55 (2019) 873–882.
[41] P. Liu, L.-N. Jin, C. Jin, J.-N. Zhang, S.-W. Bian, Synthesis of hierarchically porous silicate-1 and ZSM-5 by hydrothermal transformation of SiO2 colloid crystal/carbon composites, Microporous Mesoporous Mater. 262 (2018) 217–226.
[42] F.L. Bleken, S. Chavan, U. Olsbye, M. Boltz, F. Ocampo, B. Louis, Conversion of methanol into light olefins over ZSM-5 zeolite: Strategy to enhance propene selectivity, Appl. Catal. A 447–448 (2012) 178–185.
[43] S.K. Saxena, N. Viswanadham, Hierarchically nano porous nano crystalline ZSM-5 for improved alkylation of benzene with bio-ethanol, Appl. Mater. Today 5 (2016) 25–32.
[44] S. Jiang, H. Zhang, Y. Yan, X. Zhang, Stability and deactivation of Fe-ZSM-5 zeolite catalyst for catalytic wet peroxide oxidation of phenol in a membrane reactor, RSC Adv. 5 (2015) 41269–41277.
[45] K. Khaledi, M. Haghighi, P. Sadeghpour, On the catalytic properties and performance of core-shell ZSM-5@MnO nanocatalyst used in conversion of methanol to light olefins, Microporous Mesoporous Mater. 246 (2017) 51–61.
[46] P. Sadeghpour, M. Haghighi, DEA/TEAOH templated synthesis and characterization of nanostructured NiAPSO-34 particles: Effect of single and mixed templates on catalyst properties and performance in the methanol to olefin reaction, Particuology 19 (2015) 69–81.
[47] J.S. Martinez-Espin, M. Morten, T.V.W. Janssens, S. Svelle, P. Beato, U. Olsbye, New insights into catalyst deactivation and product distribution of zeolites in the methanol-to-hydrocarbons (MTH) reaction with methanol and dimethyl ether feeds, Catal. Sci. Technol. 7 (2017) 2700–2716.
[48] J. Zhang, H. Zhang, X. Yang, Z. Huang, W. Cao, Study on the deactivation and regeneration of the ZSM-5 catalyst used in methanol to olefins, J. Nat. Gas Chem. 20 (2011) 266–270.
[49] H. An, F. Zhang, Z. Guan, X. Liu, F. Fan, C. Li, Investigating the Coke Formation Mechanism of H-ZSM-5 during Methanol Dehydration Using Operando UV–Raman Spectroscopy, ACS Catal. 8 (2018) 9207–9215.